

# The Planetary Nebula Luminosity Function

Robin Ciardullo

The Pennsylvania State University, Department of Astronomy and Astrophysics 525  
Davey Lab University Park, PA 16803, USA

**Abstract.** The [O III]  $\lambda 5007$  planetary nebula luminosity function (PNLF) occupies an important place on the extragalactic distance ladder: it is the only standard candle that can be applied to all the large galaxies of the Local Supercluster. We review the method's precision, and use it to show that the distance scale defined by Cepheids and the Surface Brightness Fluctuation method is likely too large by  $\sim 7\%$ . We also discuss some of the physics underlying the phenomenon, and present clues as why the technique is so resilient.

## 1 Introduction

Planetary nebulae (PNe) are unique probes of galactic chemical and dynamical evolution. But before they can be used, they must be found, and the best way of doing this involves searching for PN candidates via their bright [O III]  $\lambda 5007$  emission. As a result, the first piece of information obtained about a set of extragalactic PNe is their [O III]  $\lambda 5007$  luminosity function. Since this luminosity function contains information about both distance and parent population, one should make every effort to understand its properties and features.

## 2 The PN Luminosity Function as a Distance Indicator

Although the idea of using PNe as extragalactic distance indicators was first suggested in the early 1960's [1,2], it was not until the late 1970's that a PN-based distance estimate was made [3], and the first study of the [O III]  $\lambda 5007$  planetary nebula luminosity function (PNLF) was not performed until 1989 [4,5]. In fact, it is an irony of the subject that PN distance measurements inside the Local Group [6] were made only after the technique had been applied to more distant systems [3,7], and the first application of the PNLF inside the Milky Way [8] occurred after the method had been used to estimate the Hubble Constant [9]. This odd chronology, of course, was due to the fact that individual PNe are definitely not standard candles [10,11,12], and that distance estimates to Galactic PNe are extremely poor. Nevertheless, today the [O III]  $\lambda 5007$  PNLF is one of the most important standard candles in extragalactic astronomy, and the only method that can be applied to all the large galaxies of the Local Supercluster, regardless of environment or Hubble type (see Fig. 1).

The use of the PN luminosity function is extremely simple. One surveys a distant galaxy or cluster and identifies point sources that are present in [O III]

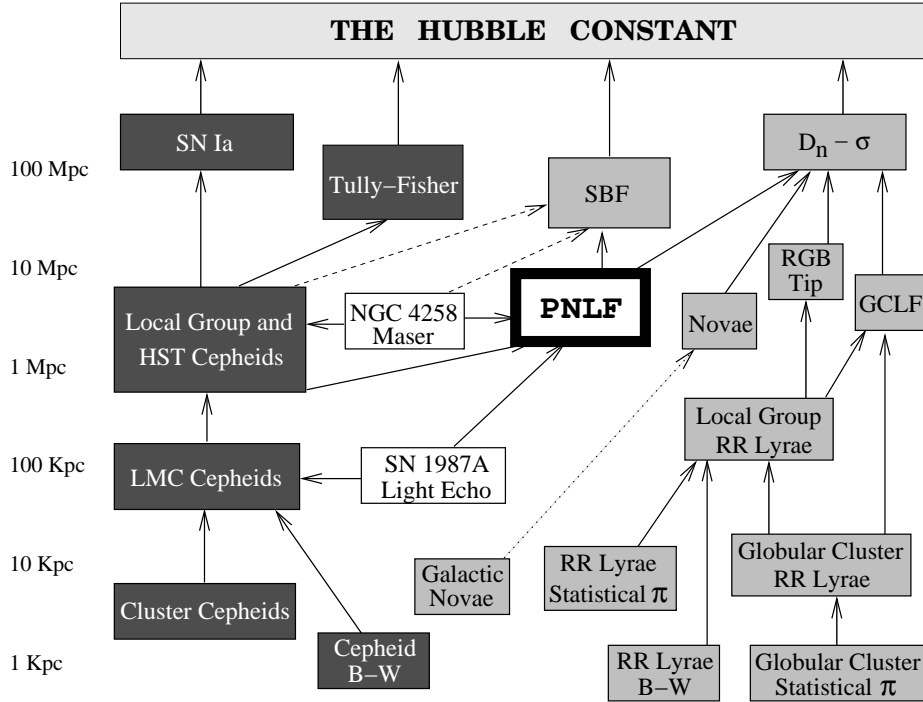


**Fig. 1.** The extragalactic distance ladder. The dark boxes show techniques useful in star-forming galaxies, the lightly-filled boxes give methods that work in Pop II systems, and the open boxes represent geometric distance determinations. Uncertain calibrations are noted as dashed lines. The PNLF is the only method that is equally effective in all the populations of the Local Supercluster.

$\lambda 5007$  but completely invisible in the continuum. These are the planetary nebula candidates. Unfortunately, mixed in with the PNe are three types of contaminants:

*H II Regions:* Star formation is not an issue in most elliptical and lenticular galaxies, but in late-type systems, the H II regions around O and B stars will far outnumber the PNe. Fortunately, most H II regions are resolvable under good seeing ( $\lesssim 1''$ ) conditions, and their exciting stars may be visible on deep continuum images. This contrasts with PNe which (in galaxies more distant than the Magellanic Clouds) are always stellar and have invisible central stars. Moreover, observations in M31's bulge, M33's disk, and the LMC have shown that all planetaries in the top  $\sim 1$  mag of the PNLF have  $[\text{O III}] \lambda 5007$  to  $\text{H}\alpha + [\text{N II}]$  line ratios greater than  $\sim 1.6$  [13]. Most H II regions have  $\text{H}\alpha$  brighter than  $[\text{O III}]$  [14].

*Supernova Remnants:* Unresolved high-excitation supernova remnants can masquerade as planetary nebulae, especially in galaxies that have a cold, high-density interstellar medium. Because compact supernova remnants are rare, their

effect on the PNLF is minimal. Nevertheless, one needs to be aware of this source of contamination, especially at the bright limit of the luminosity function. Any single object that appears overluminous in [O III]  $\lambda 5007$  could be the result of a supernova explosion.

*Ly $\alpha$  Galaxies:* At  $z = 3.12$ , Ly $\alpha$  is redshifted to 5007 Å, and at fluxes below  $\sim 10^{-16}$  ergs cm $^{-2}$  s $^{-1}$ , unresolved and marginally resolved high-redshift galaxies with extremely strong Ly $\alpha$  emission (equivalent widths  $\gtrsim 300$  Å in the observers frame) can mimic planetary nebulae [15,16]. Since the surface density of these starbursting objects is relatively low,  $\sim 1$  arcmin $^{-2}$  per unit redshift interval brighter than  $5 \times 10^{-17}$  ergs cm $^{-2}$  s $^{-1}$  [17], PN surveys in galaxies are not strongly affected by this contaminant. However, in the intracluster environment of systems such as Virgo and Fornax, Ly $\alpha$  galaxies are the predominant source of error, and they limit the effectiveness of any luminosity function analysis. To identify these interlopers, one must either obtain deep broadband images (to detect the underlying continuum of the galaxies) or perform spectroscopy (to test for the existence of [O III]  $\lambda 4959$  or resolve the  $\sim 400$  km s $^{-1}$  width of the Ly $\alpha$  line).

Once the PNe are found, all one needs to do to determine a distance is to measure their monochromatic [O III]  $\lambda 5007$  fluxes, define a statistical sample of objects, and fit the observed luminosity function to some standard law. For simplicity, Ciardullo *et al.* [5] have described the PNLF via a truncated exponential

$$N(M) \propto e^{0.307M} \{1 - e^{3(M^* - M)}\} \quad (1)$$

where

$$m_{5007} = -2.5 \log F_{5007} - 13.74 \quad (2)$$

though other forms of the relation are possible [18]. In the above equation, the key parameter is  $M^*$ , the absolute magnitude of the brightest planetary. Despite some efforts at Galactic calibrations [8,18], the PNLF remains a secondary standard candle. The original value for the zero point,  $M^* = -4.48$ , was based on an M31 infrared Cepheid distance of 710 kpc [19] and a foreground extinction of  $E(B - V) = 0.11$  [20]. Since then, M31's distance has increased [21], its reddening has decreased [23], and, most importantly, the Cepheid distances to 12 additional galaxies have been included in the calibration [13]. Somewhat fortuitously, the current value of  $M^*$  is only 0.01 mag fainter than the original value,  $M^* = -4.47 \pm 0.05$ .

Note that all PNLF distances require some estimate of the foreground interstellar extinction. There are two sources to consider. The first, extinction in the Milky Way, is readily available from reddening maps derived from H I measurements and galaxy counts [22] and/or from the DIRBE and IRAS satellite experiments [23]. The second, internal extinction in the host galaxy, is only a problem in late-type spiral and irregular galaxies. Unfortunately, it is difficult to quantify. In the Galaxy, the scale height of PNe is significantly larger than that of the dust [24]. If the same is true in other galaxies, then we would expect the bright end of the PNLF to always be dominated by objects foreground to the dust layer. This conclusion seems to be supported by observational data [25,13]

and numerical models [25], both of which suggest that the internal extinction which affects a galaxy’s PN population is  $\lesssim 0.05$  mag. We will revisit this issue in Section 3.

### 3 Tests of the Technique

In the past decade, the PNLF has been subjected to a number of rigorous tests. These tests fall into four categories.

#### 3.1 Internal Tests Within Galaxies

Five galaxies have large enough PN samples to test for radial gradients in the location of the PNLF cutoff. Two are large-bulge Sb spirals (M31 [26] and M81 [27]), one is a pure-disk Sc spiral with a strong metallicity gradient (M33 [28]), one is large elliptical galaxy (NGC 4494 [29]), and one is a blue, interacting peculiar elliptical (NGC 5128 [30]). No significant change in the PNLF has been seen in *any* of these systems. Given the diversity of the stellar populations sampled in these systems, this result, in itself, is impressive proof of the robustness of the method.

#### 3.2 Internal Tests Within Galaxy Groups

To date, six galaxy clusters have multiple PNLF measurements: the M81 Group (M81 and NGC 2403 [31,25]), the NGC 1023 Group (NGC 891 and 1023 [32]), the NGC 5128 Group (NGC 5102, 5128, and 5253 [33,30,34]), the Fornax Cluster (NGC 1316, 1380, 1399, and 1404 [35]), the Leo I Group (NGC 3351, 3368, 3377, 3379, and 3384 [13,25,36]), and the Virgo Cluster (NGC 4374, 4382, 4406, 4472, 4486, and 4649 [9]). In each system, the observed galaxies have a range of color, absolute magnitude, and Hubble type. Despite these differences, no discrepant distances have been found, as the galaxies of each group always fall within  $\sim 1$  Mpc of each other. Indeed, the PNLF measurements in Virgo easily resolve the infalling M84/M86 Group, which is background to the main body of the cluster [37].

#### 3.3 External Tests with Different Methods

Because planetary nebulae are found in all types of galaxies, it is possible to compare the results of the PNLF method directly with distances derived from all of the other techniques at the top of the distance ladder. The most instructive of these comparisons involve Cepheid variables and the Surface Brightness Fluctuation (SBF) Method.

Figure 2 compares the PNLF distances of 13 galaxies (derived using the foreground extinction estimates from DIRBE/IRAS [23]) with the final Cepheid distances produced by the *HST Key Project* [21]. Neither dataset has been corrected for the effects of metallicity. Since the absolute magnitude of the PNLF

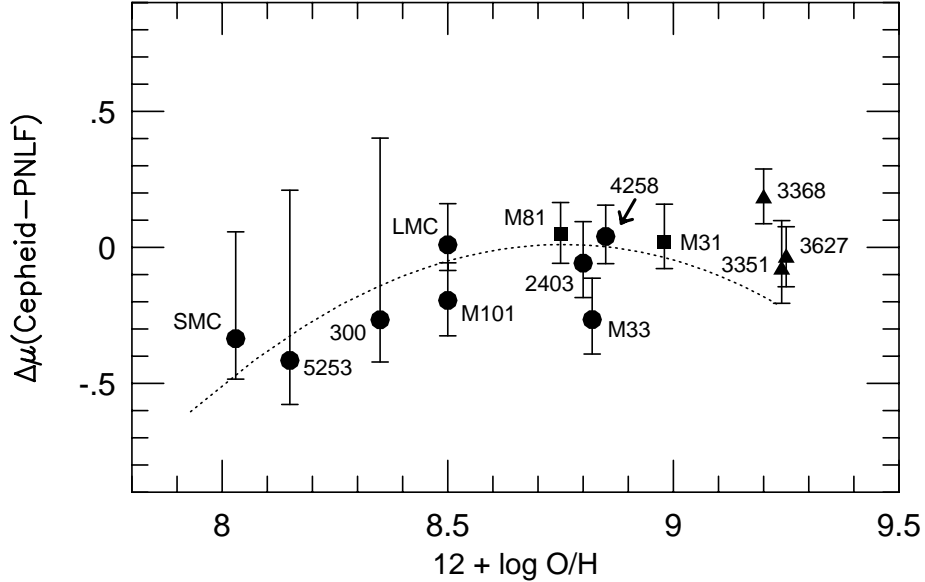


**Fig. 2.** A comparison of the PNLF and Cepheid distance moduli as function of galactic oxygen abundance, as estimated from the systems' H II regions [39]. No metallicity correction has been applied to either distance indicator. Circles represent PNLF measurements in galactic inner disks, squares in galactic bulges, and triangles in outer disks/halos. The error bars display the formal uncertainties of the methods added in quadrature; small galaxies with few PNe have generally larger errors. The curve shows the expected reaction of the PNLF to metallicity [38]. Note that metal-rich galaxies should not follow this relation, since these objects always contain enough lower metallicity stars to populate the PNLF's bright-end cutoff. The scatter between the measurements is consistent with the internal errors of the methods.

cutoff,  $M^*$ , is calibrated via these Cepheid distances, the weighted mean of the distribution must, by definition, be zero. However, the scatter about this mean, and the systematic trends in the data, are valid indicators of the reliability of the technique.

As Fig. 2 illustrates, the scatter between the Cepheid and PNLF distances is impressively small. Except for the most metal-poor systems, the residuals are perfectly consistent with the internal uncertainties of the methods. Moreover, the systematic shift seen at low-metallicity is exactly that predicted by models of post-AGB evolution [38]. There is little room for any additional metallicity term, either in the Cepheid or PNLF relations.

Figure 3 compares the PNLF distances of 29 galaxies with distances derived from SBF measurements. As is illustrated, the relative distances of the two methods are in excellent agreement: the scatter in the data is exactly that predicted from the internal errors of the measurements. However, the absolute distance scale derived from the SBF data is  $\sim 0.3$  mag larger than that inferred

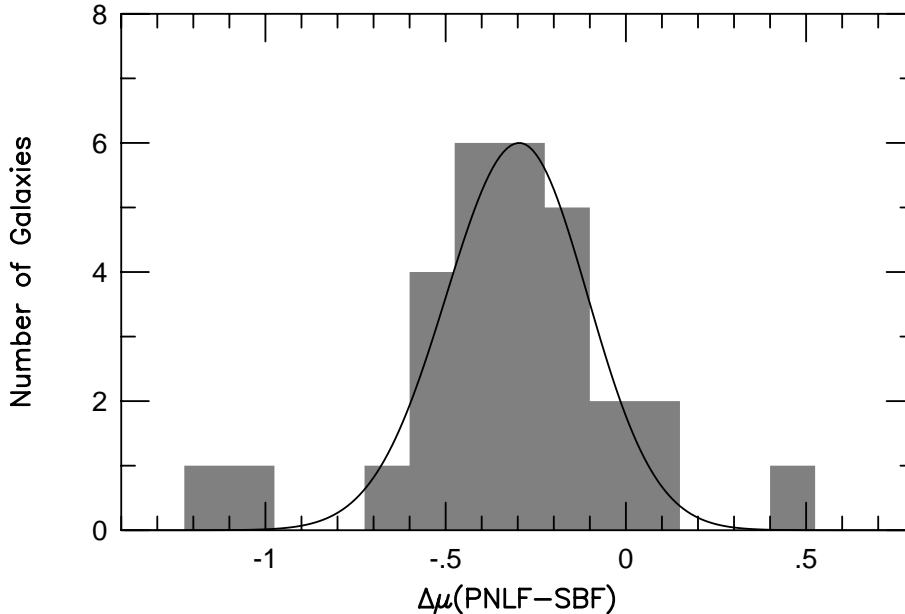


**Fig. 3.** A histogram of the difference between the PNLF and SBF distance moduli for 29 galaxies measured by both methods. The two worst outliers are the edge-on galaxies NGC 4565 ( $\Delta\mu = -0.80$ ) and NGC 891 ( $\Delta\mu = +0.71$ ). The curve represents the expected dispersion of the data. The figure demonstrates that the absolute scales of the two techniques are discrepant by  $\sim 0.3$  mag, but the internal and external errors of the methods agree.

from the PNLF. Since both techniques are calibrated via Cepheid measurements, and both have formal zero-point uncertainties of  $\sim 0.05$  mag, this type of offset should not exist.

The most likely cause of the discrepancy is a small amount of internal extinction in the Cepheid calibration galaxies. For most methods (including the PNLF), an underestimate of extinction produces an underestimate of luminosity. As a result, undetected internal extinction within a Cepheid calibration galaxy propagates into an underestimate of the standard candle's brightness, and an extragalactic distance scale that is too small. For the SBF technique, however, the opposite is true. The SBF standard candle,  $\bar{M}_I$ , is extremely sensitive to color, i.e.,

$$\bar{M}_I = -1.74 + 4.5[(V - I)_0 - 1.15] \quad (3)$$

[40]. If internal extinction exists in an SBF calibrator, the galaxy's underlying population will appear too red, and the inferred value of  $\bar{M}_I$  will be too bright. The result will be a set of distances that are systematically too large.

If internal extinction really is responsible for the offset displayed in Fig. 3, then the zero points of both systems must be adjusted. These corrections propa-

gate all the way up the distance ladder. For example, according to the *HST Key Project*, the SBF-based Hubble Constant is  $69 \pm 4$  (random)  $\pm 6$  (systematic)  $\text{km s}^{-1} \text{Mpc}^{-1}$  [21]. However, if we assume that the calibration galaxies are internally reddened by  $E(B - V) \sim 0.04$ , then the zero point of the SBF system fades by 0.17 mag, and the SBF Hubble Constant increases to  $75 \text{ km s}^{-1} \text{Mpc}^{-1}$ . This one correction is as large as the technique’s entire systematic error budget. Such an error could not have been found without the cross-check provided by PNLF measurements.

### 3.4 External Comparisons with Geometric Distances

Two galaxies have distance measurements that do not depend on the distance ladder. The first is NGC 4258, which has a resolved disk of cold gas orbiting its central black hole. The proper motions and radial accelerations of water masers associated with this gas yield an unambiguous geometric distance of  $7.2 \pm 0.3 \text{ Mpc}$  [41]. The second benchmark comes from the light echo of SN 1987A in the Large Magellanic Cloud. Although the geometry of the light echo is still somewhat controversial, the most detailed and complete analysis of the object to date gives a distance of  $D < 47.2 \pm 0.1 \text{ kpc}$  [42]. In Table 1 we compare these values with the distances determined from the PNLF [13] and from Cepheids [21].

**Table 1.** Benchmark Galaxy Distances

Method	LMC	NGC 4258	$\Delta\mu$ (mag)
Geometry	$< 18.37 \pm 0.04$	$29.29 \pm 0.09$	$10.92 \pm 0.10$
Cepheids	18.50	$29.44 \pm 0.07$	$10.94 \pm 0.07$
PNLF	$18.47 \pm 0.11$	$29.43 \pm 0.09$	$10.96 \pm 0.14$

As the table demonstrates, the Cepheid and PNLF methods both overestimate the distance to NGC 4258 by  $\sim 0.14$  mag, i.e., by  $\sim 1.3\sigma$  and  $1.1\sigma$ , respectively. In the absence of some systematic error affecting both methods, the probability of this happening is  $\lesssim 5\%$ . On the other hand, there is no disagreement concerning NGC 4258’s distance *relative to that of the LMC*: the Cepheids, PNLF, and geometric techniques all agree to within  $\pm 2\%$ ! Such a small error is probably fortuitous, but it does suggest the presence of a systematic error that affects the entire extragalactic distance ladder.

In fact, the *HST Key Project* distances are all based on an LMC distance modulus of  $(m - M)_0 = 18.50$  [21], and, via the data of Fig. 2, the PNLF distance scale is tied to that of the Cepheids. If the zero point of the Cepheid scale were shifted to  $(m - M)_0 = 18.37$ , then all the measurements would be in agreement. This consistency supports a shorter distance to the LMC, and argues for a 7% increase in the *HST Key Project* Hubble Constant to  $77 \text{ km s}^{-1} \text{Mpc}^{-1}$ .

## 4 The Physics of the Luminosity Function

The fact that the PNLF method is insensitive to metallicity is not a surprise. Since oxygen is a primary nebular coolant, any decrease in its abundance raises the plasma's electron temperature and increases the rate of collisional excitations per ion. This mitigates the effect of having fewer emitting ions in the nebula, so that a decrease in oxygen abundance only lessens the emergent [O III]  $\lambda 5007$  line flux by (roughly) the square root of the abundance difference [4]. Meanwhile, the PN's core reacts to metallicity in the opposite manner. If the metallicity of the progenitor star is decreased, then the PN's central star will be slightly more massive and its emergent UV flux will be slightly greater [43,44]. This additional energy almost exactly compensates for the decreased emissivity of the nebula. As a result, the total [O III]  $\lambda 5007$  flux that is generated by a planetary is virtually independent of metallicity. This fortuitous cancellation has been confirmed by more detailed models of PN evolution: only in the most metal-poor systems does the brightness of the PNLF cutoff fade by more than a few percent [38].

The insensitivity of the PNLF cutoff to population age is more difficult to understand. A PN's [O III]  $\lambda 5007$  flux is directly proportional to the luminosity of its central star, and this luminosity, in turn, is extremely sensitive to central star mass [45,46]. Since central star mass is directly proportional to progenitor mass via the initial mass-final mass relation [47], one would think that the PNLF cutoff would fade dramatically with time [48]. Yet observations demonstrate that this fading does not occur.

Although we do not as yet have a complete theory for the age-invariance of the PNLF, a few clues are beginning to emerge. The first concerns the faint end of the luminosity function. Although the location of the PNLF cutoff does not change with stellar population, the same is not true for the function's overall shape. As Fig. 4 demonstrates, old populations, such as M31's bulge, have a PNLF that increases exponentially following  $N(m) \propto e^{0.307m}$ . This type of behavior is expected if the PNe of these systems have low-mass cores, so that the timescale for central star evolution is much longer than that for nebular expansion [1,28]. In contrast, star-forming galaxies have a "dip" in the PNLF at magnitudes between  $\sim 2$  and  $\sim 4$  mag down from  $M^*$ . This deficit is a natural characteristic of models in which the evolution of [O III]  $\lambda 5007$  is governed by the rapid evolution of a high-mass core. In such systems, the non-monotonic PNLF is simply a reflection of the bimodal luminosity function expected from post-AGB stars [45].

A second clue to the PNLF comes from the fortuitous correlation between the maximum UV emission achieved by a PN central star and the mass of its envelope. High luminosity PN cores have large circumstellar envelopes, and, consequently, large amounts of circumstellar dust. The extinction caused by this dust can act to regulate the amount of [O III]  $\lambda 5007$  flux generated by a planetary, so that the luminosity of high core-mass objects never exceeds  $M^*$ . Support for this scenario comes from the fact that nine Magellanic Cloud planetaries have intrinsic [O III]  $\lambda 5007$  magnitudes brighter than  $M^*$ , but *all* are self-extincted below the PNLF cutoff [49,50,51]. In addition, there is observational evidence

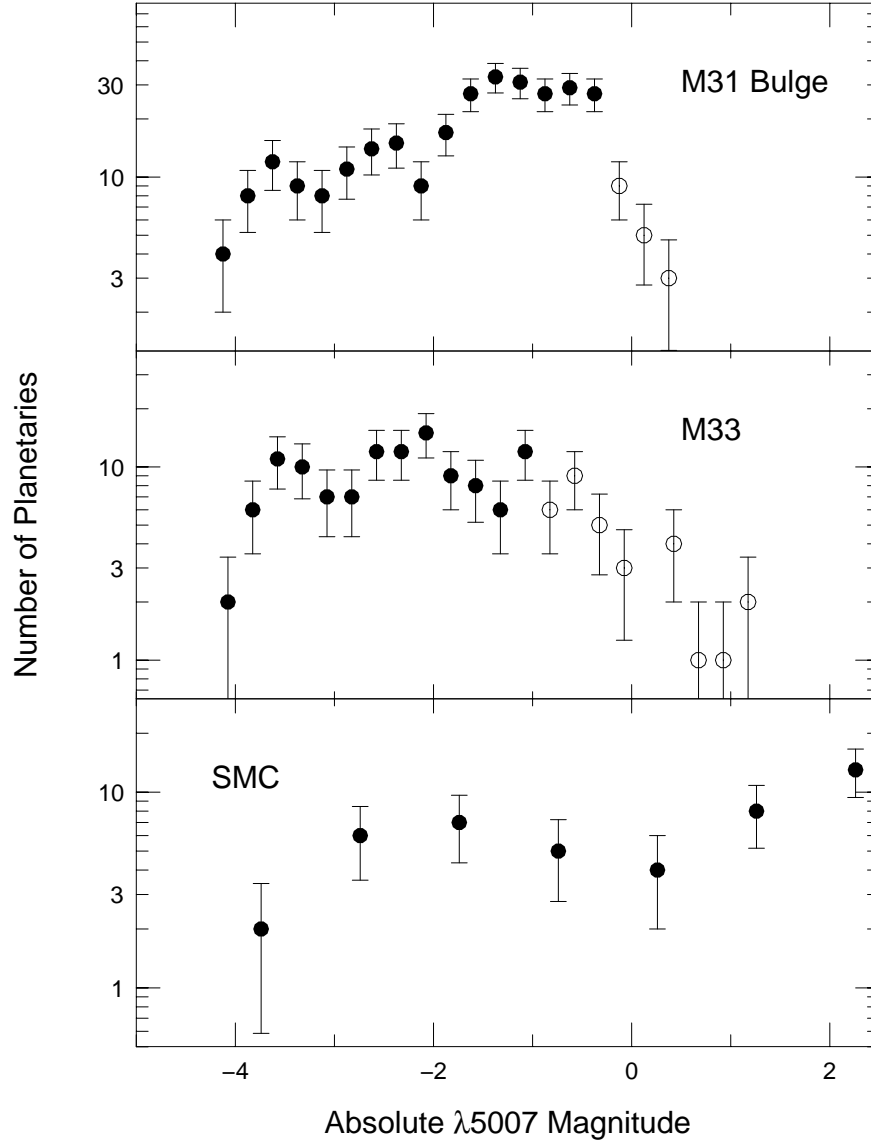


**Fig. 4.** The [O III]  $\lambda 5007$  planetary nebula luminosity functions of three Local Group stellar populations. Old populations, such as that found in the bulge of M31, have an exponentially increasing PNLf. In contrast, the PNLFs of star-forming systems are non-monotonic, with a “dip” that begins  $\sim 2$  mag below  $M^*$ . The location of this dip is consistent with models in which the luminosity evolution of planetary nebulae is governed by the rapid evolution of high-mass central stars.

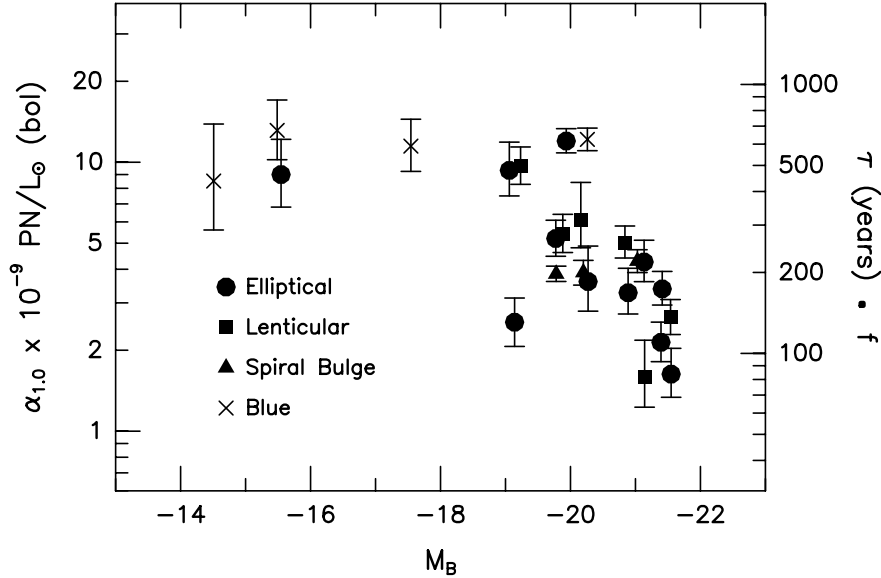


**Fig. 5.** The bolometric luminosity-specific number of PNe in the top 1 mag of the [O III]  $\lambda 5007$  PNLF plotted as a function of galactic absolute  $B$  magnitude. The right side of the  $y$ -axis translates this number into a constraint on the PN lifetime using a luminosity-specific stellar evolutionary flux of  $2 \times 10^{-11}$  stars  $\text{yr}^{-1} L_{\odot}$ . Either the [O III]-bright PNe of giant ellipticals live very short lives, or a substantial fraction of the stars in these galaxies do not contribute to the bright-end of the PNLF.

for a correlation between the amount of PN circumstellar extinction and central star mass for young, [O III]-bright objects [52].

The final constraint on the physics of the PNLF comes from the number of PN produced by different stellar populations. According to the theory of stellar energy generation [53], all populations older than  $\sim 1$  Gyr create  $\sim 1$  PN per year per  $5 \times 10^{12} L_{\odot}$  (bolometric). If this is true, then measurements of the luminosity-specific number of PNe present in a galaxy can be immediately translated into constraints on the lifetime of an [O III]-bright nebula and on the fraction of stars which go through the bright planetary nebula phase.

This constraint is given in Fig. 5. For small and medium-sized galaxies, PNe typically spend  $\sim 500$  yr within  $\sim 1$  mag of  $M^*$ . However, the apparent PN timescale decreases dramatically for objects in giant elliptical and lenticular galaxies. Either the [O III]-bright planetaries in these systems have much shorter lives than their small-galaxy counterparts, or a substantial fraction of the stars of giant ellipticals do not evolve into these types of objects.

## 5 The Future

Of course, attempting to derive the evolution of ensembles of planetary nebulae from [O III] data alone is like trying to infer the evolution of star clusters from photometry performed through only one filter. In order to gain a fuller understanding of the global properties of planetary nebulae, one must study the luminosity function of PNe in a multi-dimensional emission-line space. The data for such a study are just now beginning to be available. Narrow-band photometric surveys are yielding information on the absolute line strengths of PNe in [O III]  $\lambda 5007$  and  $H\alpha + [\text{N II}]$  for a variety of stellar populations. Follow-up radial velocity surveys are then producing data on  $H\beta$  relative to [O III]  $\lambda 5007$  and, in some cases, [N II] and [S II] relative to  $H\alpha$ . By comparing these measurements to models, we should be able to gain a much more complete understanding of planetary nebula phenomenon.

This work was supported in part by NSF grant AST 00-71238.

## References

1. K.G. Henize, B.E. Westerlund: *Ap. J.* **137**, 747 (1963)
2. P.W. Hodge: *Galaxies and Cosmology*. (McGraw-Hill, New York 1966)
3. H.C. Ford, D.C. Jenner: *Bull. A.A.S.* **10**, 665 (1978)
4. G.H. Jacoby: *Ap. J.* **339**, 39 (1989)
5. R. Ciardullo, G.H. Jacoby, H.C. Ford, J.D. Neill: *Ap. J.* **339**, 53 (1989)
6. G.H. Jacoby, M.P. Lesser: *A. J.* **86**, 185 (1981)
7. D.G. Lawrie, J.A. Graham: *Bull. A.A.S.* **15**, 907 (1983)
8. S.R. Pottasch: *Astr. Ap.* **236**, 231 (1990)
9. G.H. Jacoby, R. Ciardullo, H.C. Ford: *Ap. J.* **356**, 332 (1990)
10. L. Berman: *Lick Obs. Bull.* **18**, 57 (1937)
11. R. Minkowski: *Pub. Obs. Univ. Mich.* **10**, 25 (1951)
12. I.S. Shkolovski: *Astron. Zh.* **33**, 222 (1956)
13. R. Ciardullo, J.J. Feldmeier, G.H. Jacoby, R.K. de Naray, M.B. Laychak, P.R. Durrell: *Ap. J.* **577**, 31 (2002)
14. P.A. Shaver, R.X. McGee, L.M. Newton, A.C. Danks, S.R. Pottasch: *M.N.R.A.S.* **204**, 53 (1983)
15. R.-P. Kudritzki, R.H. Méndez, J.J. Feldmeier, R. Ciardullo, G.H. Jacoby, K.C. Freeman, M. Arnaboldi, M. Capaccioli, O. Gerhard, H.C. Ford: *Ap. J.* **536**, 19 (2000)
16. K.C. Freeman, M. Arnaboldi, M. Capaccioli, R. Ciardullo, J. Feldmeier, H. Ford, O. Gerhard, R. Kudritzki, G. Jacoby, R.H. Méndez, R. Sharples: 'Intracluster Planetary Nebulae in the Virgo Cluster'. In: *Dynamics of Galaxies: From the Early Universe to the Present, ASP Conference 197*, ed. by F. Combes, G.A. Mamom, V. Charmandaris (Astronomical Society of the Pacific, San Francisco 2000) pp. 389-392
17. R. Ciardullo, J.J. Feldmeier, K. Krelow, G.H. Jacoby, C. Gronwall: *Ap. J.* **566**, 784 (2002)
18. R.H. Méndez, R.P. Kudritzki, R. Ciardullo, G.H. Jacoby: *Astr. Ap.* **275**, 534 (1993)

19. D.L. Welch, C.W. McAlary, R.A. McLaren, B.F. Madore: *Ap. J.* **305**, 583 (1986)
20. R.D. McClure, R. Racine: *A. J.* **74**, 1000 (1969)
21. W.L. Freedman, B.F. Madore, B.K. Gibson, L. Ferrarese, D.D. Kelson, S. Sakai, J.R. Mould, R.C. Kennicutt, Jr., H.C. Ford, J.A. Graham, J.P. Huchra, S.M.G. Hughes, G.D. Illingworth, L.M. Macri, P.B. Stetson: *Ap. J.* **553**, 47 (2001)
22. D. Burstein, C. Heiles: *Ap. J. Suppl.* **54**, 33 (1984)
23. D.J. Schlegel, D.P. Finkbeiner, M. Davis: *Ap. J.* **500**, 525 (1998)
24. D. Mihalas, J. Binney: *Galactic Astronomy*. (W.H. Freeman, New York 1981)
25. J.J. Feldmeier, R. Ciardullo, G.H. Jacoby: *Ap. J.* **479**, 231 (1997)
26. X. Hui, H. Ford, G. Jacoby: *Bull.A.A.S.* **26**, 938 (1994)
27. L. Magrini, M. Perinotto, R.L.M. Corradi, A. Mampaso: *Astr. Ap.* **379**, 90 (2001)
28. R. Ciardullo, P.R. Durrell, M.B. Laychak, K.A. Herrmann, K. Moody, G.H. Jacoby, J.J. Feldmeier: *Ap. J.* in press
29. G.H. Jacoby, R. Ciardullo, W.E. Harris: *Ap. J.* **462**, 1 (1996)
30. X. Hui, H.C. Ford, R. Ciardullo, G.H. Jacoby: *Ap. J.* **414**, 463 (1993)
31. G.H. Jacoby, R. Ciardullo, H.C. Ford, J. Booth: *Ap. J.* **344**, 704 (1989)
32. R. Ciardullo, G.H. Jacoby, W.E. Harris: *Ap. J.* **383**, 487 (1991)
33. R. McMillan, R. Ciardullo, G.H. Jacoby: *A. J.* **108**, 1610 (1994)
34. M.M. Phillips, G.H. Jacoby, A.R. Walker, J.L. Tonry, R. Ciardullo: *Bull. A.A.S.* **24**, 749 (1992)
35. R. McMillan, R. Ciardullo, G.H. Jacoby: *Ap. J.* **416**, 62 (1993)
36. R. Ciardullo, G.H. Jacoby, H.C. Ford: *Ap. J.* **344**, 715 (1989)
37. H. Böhringer, U.G. Briel, R.A. Schwarz, W. Voges, G. Hartner, J. Trümper: *Nature* **368**, 828 (1994)
38. M.A. Dopita, G.H. Jacoby, E. Vassiliadis: *Ap. J.* **389**, 27 (1992)
39. L. Ferrarese, H.C. Ford, J. Huchra, R.C. Kennicutt, J.R. Mould, S. Sakai, W.L. Freedman, P.B. Stetson, B.F. Madore, B.K. Gibson, J.A. Graham, S.M. Hughes, G.D. Illingworth, D.D. Kelson, L. Macri, K. Sebo, N.A. Silbermann: *Ap. J. Suppl.* **128**, 431 (2000)
40. J.L. Tonry, A. Dressler, J.P. Blakeslee, E.A. Ajhar, A.B. Fletcher, G.A. Luppino, M.R. Metzger, C.B. Moore: *Ap. J.* **546**, 681 (2001)
41. J.R. Herrnstein, J.M. Moran, L.J. Greenhill, P.J. Diamond, M. Inoue, N. Nakai, M. Miyoshi, C. Henkel, A. Riess: *Nature* **400**, 539 (1999)
42. A. Gould, O. Uza: *Ap. J.* **494**, 118 (1998)
43. J.C. Lattanzio: *Ap. J.* **311**, 708 (1986)
44. E. Brocato, F. Matteucci, I. Mazzitelli, A. Tornabé: *Ap. J.* **349**, 458 (1990)
45. E. Vassiliadis, P.R. Wood: *Ap. J. Suppl.* **92**, 125 (1994)
46. T. Blöcker: *Astr. Ap.* **299**, 755 (1995)
47. V. Weidemann: *Astr. Ap.* **363**, 647 (2000)
48. P. Marigo, L. Girardi, A. Weiss, M.A.T. Groenewegen, C. Chiosi: *Astr. Ap.*, in press
49. S.J. Meatheringham, M.A. Dopita: *Ap. J. Suppl.* **75**, 407 (1991)
50. S.J. Meatheringham, M.A. Dopita: *Ap. J. Suppl.* **76**, 1085 (1991)
51. G.H. Jacoby, A.R. Walker, R. Ciardullo: *Ap. J.* **365**, 471 (1990)
52. R. Ciardullo, G.H. Jacoby: *Ap. J.* **515**, 191 (1999)
53. A. Renzini, A. Buzzoni: In: *Spectral Evolution of Galaxies*, ed. by C. Chiosi, A. Renzini (Reidel, Dordrecht), p. 195 (1986)